

Japan's south foehn on the Toyama Plain: Dynamical or thermodynamical mechanisms?

Hiroyuki Kusaka¹  | Akifumi Nishi^{1,2} | Ai Kakinuma^{3,4} |
Quang-Van Doan¹  | Taira Onodera³ | Shuhei Endo³

¹Center for Computational Sciences,
University of Tsukuba, Tsukuba, Japan

²National Defense Academy of Japan,
Yokosuka, Japan

³Graduate School of Life and
Environmental Sciences, University of
Tsukuba, Tsukuba, Japan

⁴Japan Weather Association, Tokyo, Japan

Correspondence

Hiroyuki Kusaka, Center for
Computational Sciences, University of
Tsukuba, 1-1-1 Tennoudai, Tsukuba,
Ibaraki 305-8577, Japan.
Email: kusaka@ccs.tsukuba.ac.jp

Funding information

Environmental Restoration and
Conservation Agency of Japan, Grant/
Award Number: JPMEERF20192005; New
Energy and Industrial Technology
Development Organization, Grant/Award
Number: R&D project for technology;
Cabinet Office, Government of Japan,
Grant/Award Number: Strategic
Innovation Promotion (SIP)

Abstract

Japanese society has recently taken a greater interest in foehn warming because it has caused record-breaking high temperatures and sudden damage to rice crops. This is the first comprehensive climatological study focused on Japan's south foehn, which blows across the Toyama Plain in the Hokuriku region. Climatological analyses, including an objective self-organizing map and subjective analysis of 198 south foehn cases, revealed that ~68.2% of the foehns occurred while an extratropical cyclone was passing through the Sea of Japan. Approximately 19.7% of the remaining foehns blew while an anticyclone covered Japan. Only 5.1% of all foehns occurred during a typhoon, but very high temperatures occurred when typhoons were approaching. Foehns were observed in all seasons but tended to blow more often in spring, when there are many migratory anticyclones and cyclones. Most of the foehns begin at night and end or pause during the day. This is due to the removal of the nocturnal stable layer and the development of a local daytime pressure gradient on the lee side. The dynamical mechanism provides the primary explanation for Japan's south foehn. Surprisingly, the foehns with precipitation on windward mountains slopes accounted for only ~19.2% of all cases, with ~40.0% being typhoon cases. Most of these are likely of multiple type; a pure thermodynamical type of foehn is a rare occurrence. Numerical simulations and back trajectory analyses for 76 selected foehn cases revealed that the majority of the air parcels originated from the south and passed straight over the Hida Highlands, between two mountain ranges, as a hybrid type of gap and foehn winds.

KEYWORDS

back trajectory analysis, downslope wind, foehn warming, Hokuriku region, local winds, self-organizing map analysis, south foehn, Weather Research and Forecasting model

This is an open access article under the terms of the Creative Commons Attribution License, which permits use, distribution and reproduction in any medium, provided the original work is properly cited.

© 2021 The Authors. *International Journal of Climatology* published by John Wiley & Sons Ltd on behalf of Royal Meteorological Society.

1 | INTRODUCTION

Japanese society has recently taken a greater interest in foehn warming. This increased interest began with the 2007 revision of Japan's daily maximum temperature record for the first time in 74 years (Takane and Kusaka, 2011). In 2018, the record was broken again due to foehn warming (Nishi and Kusaka, 2019). Extremely high-temperature, nocturnal events in Niigata Prefecture in 2018 were also caused by foehn warming (Nishi *et al.*, 2019). In Japan, dry, strong, nocturnal foehn winds cause rice crops to suffer from lower the grain quality and yield (e.g., Muramatsu, 1976; Wada *et al.*, 2011).

The term “foehn” originated from the name of a local wind blowing across the European Alps, but today it is a generic term for any warm, dry, wind descending over the lee side of a mountain. Local winds similar to foehns occur worldwide; a particularly famous example is the chinook, which blows downwind over the Rocky Mountains (Brinkmann, 1974). Studies on the Alps foehn and chinook have a long history, and several mechanisms have been proposed to explain foehn warming. Among the well-known warming mechanisms, the dynamical warming mechanism (type I) and thermodynamical warming mechanism (type II) are the most prominent (Hann, 1866; see also Barry, 2008; Beran, 1967; Richiner and Hächler, 2013). The type I mechanism involves adiabatic compression warming due to downslope winds. It is also called the “isentropic drawdown” mechanism (Elvidge and Renfrew, 2016). Type II is the most well-known mechanism because it is often introduced in many meteorology textbooks. In this type, precipitation and latent heating over the windward slopes of mountains play an important role in warming. Other mechanisms have also been proposed, including that of Beran (1967), who identified two further mechanisms of warming; in these type III and IV mechanisms, it is important to remove the cold air mass and prevent nocturnal radiative cooling of the surface layer, respectively.

As the performances of numerical models and computers have improved, other mechanisms of foehn warming during precipitation events over the windward slopes of the mountains have been proposed in recent studies—“multiple mechanism” (also known as hybrid mechanism) (Takane *et al.*, 2015) and “scrambling mechanism” (Miltenberger *et al.*, 2016). The multiple mechanism is characterized as the simultaneous occurrence of the dynamical and thermodynamical mechanisms. The scrambling mechanism is similar to the multiple mechanism, but it is more sophisticated including a vertical scrambling of air mass over the mountains. Takane *et al.* (2015) was able to quantitatively distinguish between dynamical and thermodynamical warming.

Furthermore, Elvidge and Renfrew (2016) were able to quantitatively assign foehn warming to particular mechanisms (isentropic drawdown, latent heating and precipitation, and turbulent mixing of sensible heat) using high resolution simulations and back trajectory analysis.

Additionally, Takane and Kusaka (2011) and Elvidge and Renfrew (2016) respectively showed the importance of the sensible heat flux from mountain surfaces and the upper convective layer for foehn warming without precipitation. Other mechanisms were described by Richiner and Hächler (2013).

While there are various mechanisms that may underly foehn warming, the primary one may differ among regions. For example, dynamical mechanisms more frequently underly the Austrian foehn than thermodynamical mechanisms (Seibert, 1990; Würsch and Sprenger, 2015). In contrast, the Swiss foehn is more clearly characterized by thermodynamical processes, though both types occur (Würsch and Sprenger, 2015; Miltenberger *et al.*, 2016).

Past studies on foehn-type winds in various regions have indicated that characteristics such as the most favourable synoptic patterns, flow patterns, and interactions with cold pools, as well as thermally driven meso-scale circulations, differ between the various types of foehns, including the south and north foehns in the Alps (e.g., Hoinka, 1985a, 1985b; Zängl, 2003, 2004; Gohm and Mayr, 2004; Jaubert *et al.*, 2005; Drobinski *et al.*, 2007; Richiner and Hächler, 2013; Cetti *et al.*, 2015; Haid *et al.*, 2020), chinook in the Rocky Mountains (Brinkmann, 1973, 1974; Whiteman and Whiteman, 1974; Lilly, 1978; Durran, 1986), Santa Ana in California (Raphael, 2003; Hughes and Hall, 2010; Guzman-Morales *et al.*, 2016; Rolinski *et al.*, 2019), the New Zealand foehn (McGowan and Sturman, 1996; McGowan *et al.*, 2002), and the Antarctic Peninsula foehns (Orr *et al.*, 2008; Elvidge *et al.*, 2016, 2020; Turton *et al.*, 2018). Japanese foehns are not as well studied as those in the Alps, the chinook, the Santa Ana, or the Antarctic Peninsula foehn. However, some headway has been made in previous studies to understand these winds.

Foehn-type winds blow in various places across Japan (Yoshino, 1975; Kusaka and Fudeyasu, 2017). The north-west foehn that blows across the Kanto Plain in summer blows weakly under the influence of the Pacific High, and foehn warming is caused by a combination of adiabatic compression heating and surface sensible heating (Takane and Kusaka, 2011; Nishi and Kusaka, 2019).

The south foehn blows across the Sea of Japan side of Honshu (main island of Japan) (Arakawa *et al.*, 1982; Nishi *et al.*, 2019), Hokkaido (Mori and Sato, 2014), and Shikoku (Saito and Ikawa, 1993; Saito, 1994). The south foehn on the Hokuriku region in Honshu is the

representative foehn in Japan. Here, the Hokuriku region is located in the Sea of Japan side in the middle part of Honshu (Figure 1). The south foehn is often observed at the exits of valleys in the plains of Hokuriku region (A–C in Figure 1b and Figure 2) and sometimes blows strongly. For example, the speed of the “Inami-Kaze” (winds in the Inami area) blowing in Tonami Plain can be more than $50 \text{ m}\cdot\text{s}^{-1}$ (Koyanagi and Kusaka, 2019). It is also known that the south foehn in the Hokuriku region blows when an extratropical cyclone passes through the Sea of Japan or when a typhoon approaches Japan (Yoshino, 1975; Arakawa *et al.*, 1982; Shibata *et al.*, 2010). As in other areas that experience foehns, when wind direction changes rapidly to the south, wind speed increases, and temperature increases simultaneously, and relative humidity changes at almost the same time (Figure 3). However, it remains unknown whether the foehn blows under other pressure patterns.

South foehn warming may be explained by two types of warming mechanisms—those governed by dynamical and thermodynamical mechanisms (Arakawa *et al.*, 1982). However, which is the primary type is unknown, and only a few studies have been conducted on the path of Japan's south foehn (e.g., Arakawa *et al.*, 1982; Ishizaki and Takayabu, 2009; Nishi *et al.*, 2019). Arakawa *et al.* (1982) plotted the distribution of observed surface winds and conjectured that a representative south foehn on the Toyama Plain (B in Figure 1b) blows due-northward from the Nobi Plain (D in Figure 1b) to the Toyama Plain through the Hida

Highlands. Here, the Hida Highlands is the high altitude area between the Ryohaku Mountains (F in Figure 1b) and Hida Mountains (G in Figure 1b), indicating that the Highlands could play a role as the saddle, pass, or valley of the mountain range. Ishizaki and Takayabu (2009) simulated two typical south foehns and supported this proposal. However, only case studies have been employed, while determining the primary path requires more detailed numerical simulations and statistical analyses. As climatological studies on Japan's south foehn are lacking, there are still many unknown aspects of these winds, such as:

1. Are dynamical or thermodynamical mechanisms more typical of Japan's south foehn warming?
2. Does the south foehn only occur when a cyclone or typhoon approaches?
3. What is the primary path of the south foehn?

The purpose of this study is to answer these fundamental questions in order to reveal the general characteristics representative of the south foehn on the Toyama Plain in Hokuriku.

The south foehn on the Toyama Plain is called “Jintsu-Oroshi”, in reference to the downslope windstorms blowing in the Jintsu River area. This study is the first comprehensive climatological study of Japan's south foehn. As noted by Richiner and Hächler (2013), insights into natural processes can be gained by statistical analyses of many scenarios, as well as through detailed case studies.

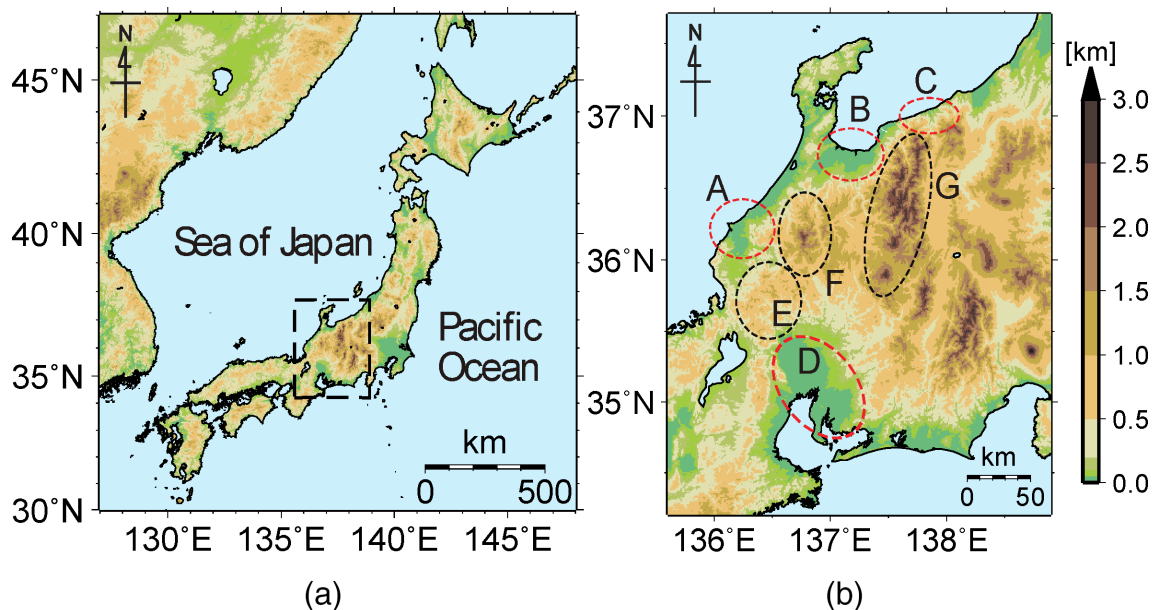


FIGURE 1 (a) Topography around the main island of Japan (i.e., Honshu). (b) Central region of Honshu. The area near the coast of the sea of Japan in (b) corresponds to the Hokuriku region. The red circles, A, B, C, and D, represent the Fukui Plain, Toyama Plain, Itoigawa Area, and the Nobi Plain, respectively. The black circles, E–G represent the Ibuki Mountains, Ryohaku Mountains, and Hida Mountains, respectively. The highlands between F and G are called the “Hida Highlands” [Colour figure can be viewed at wileyonlinelibrary.com]

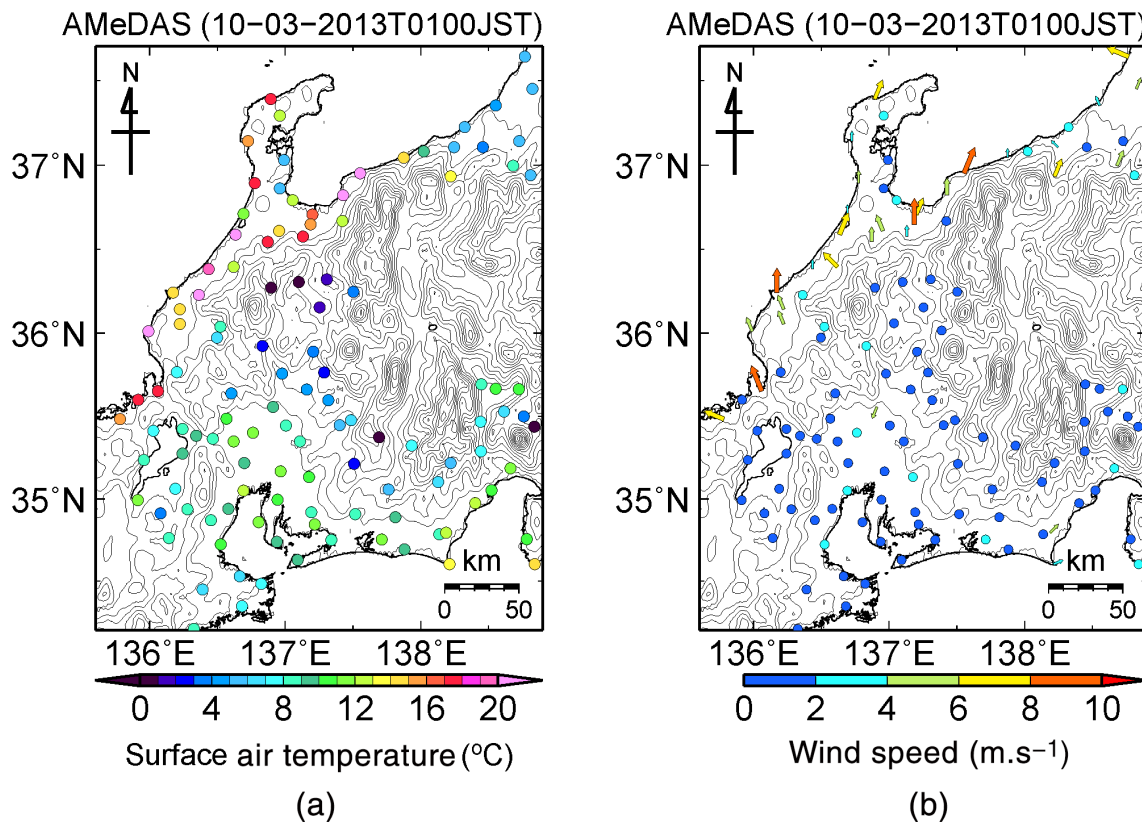


FIGURE 2 Example distributions of near-surface (a) temperatures and (b) winds obtained from observations during cyclone-induced south foehns. The solid lines indicate the topography (contour intervals of 200 m) [Colour figure can be viewed at wileyonlinelibrary.com]

2 | DATA AND METHODS

2.1 | Study area and dataset

Japan's south foehn is a downslope windstorm from the Backbone Mountain of Japan observed in the coastal areas of the Sea of Japan. It is widely known that one of the areas where the south foehn often blows is the Toyama Plain in the Hokuriku region (e.g., Arakawa *et al.*, 1982; Ishizaki and Takayabu, 2009; Shibata *et al.*, 2010). Consequently, this study was focused on the south foehn observed at the Japan Meteorological Agency (JMA) observatory in Toyama Plain. This observatory was selected as the representative observation station in the Hokuriku region, as in previous studies (c.f. Arakawa *et al.*, 1982; Ishizaki and Takayabu, 2009; Shibata *et al.*, 2010). Indeed, on days when the south foehn has been recorded at the Toyama observatory, it has usually been observed in other plains across the Hokuriku region (e.g., Arakawa *et al.*, 1982). The target period for this study lasted 10 years, from 2006 to 2015.

Surface station, radar, and operational meso-scale analysis data (MANAL), as well as surface weather charts created by the JMA were used in this study to understand the characteristics of Japan's south foehn. Here, MANAL data

have a horizontal grid spacing of 10 km (2006–2008) or 5 km (2009–2015) and a temporal resolution of 6 hr; it is created by the numerical weather prediction system using the JMA non-hydrostatic model (Saito *et al.*, 2006). The observational sampling intervals were every 10 min for surface station data, 30 min for radar data, 3 hr for objective analytical data, and 12 hr for the weather charts, respectively. The final operational analysis data (FNL) from the National Center for Environmental Prediction (NCEP) collected at a 6-hr interval were also used.

2.2 | Methodological overview

Prior to our analyses, foehns occurring between 2006 and 2015 were extracted and the typical synoptic weather patterns causing the foehn were then explored. Seasonal and daily frequencies of the foehns were surveyed, along with the intensities of foehn warming. In this study, the intensity was defined by the differences between the potential temperatures recorded at the Toyama observatory and those from an observatory on the windward plain. The wind speed during the foehns was also surveyed. We classified 198 foehn warming events as either dynamical, thermodynamical, and

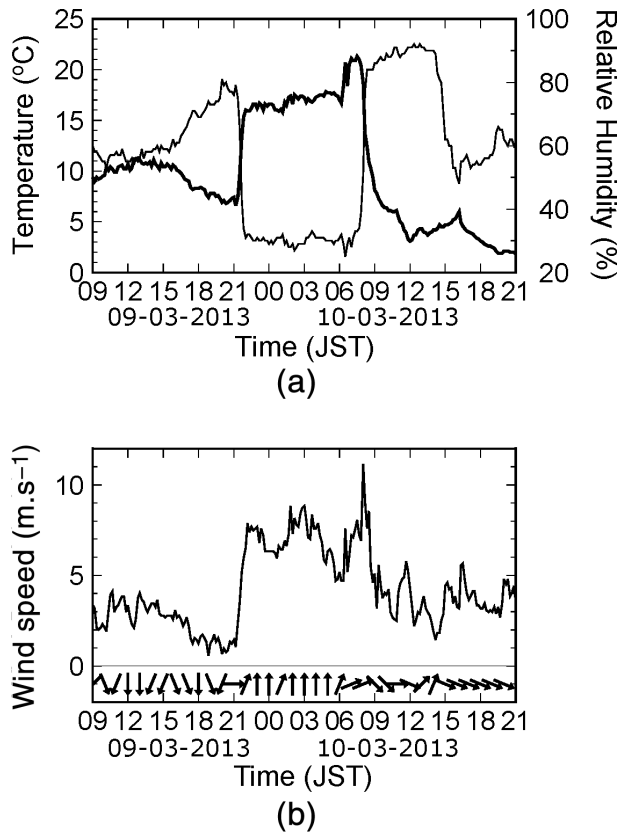


FIGURE 3 Specific example of a time series of (a) temperature and relative humidity and (b) wind speed and direction near the surface at the Toyama observatory for cyclone-induced foehns. Thick and thin lines in (a) indicate temperature and relative humidity, respectively. Solid line and vector in (b) indicate wind speed and wind direction, respectively

multiple mechanism types according to radar, rain gauge, and back trajectory analysis data in order to understand the primary mechanism driving foehn warming. Finally, typical paths of the foehn flow were investigated.

2.3 | Selection of foehns

Previously, researchers have proposed selection methods, definitions, and indices for the Alps foehn (e.g., Drechsel and Mayr, 2008; Mayr *et al.*, 2018). While these methods are beneficial, they are not desirable for application to Japan's south foehn because of its local characteristics. In a previous study on Japan's south foehn, high-temperature and low-humidity days, when winds were blowing from the direction of the mountains, were regarded as foehn occurrence days (Shibata *et al.*, 2010). However, in this simplified approach, there is a possibility that hot and dry days caused by changes in large-scale phenomena may also be regarded as foehn occurrence

days. As Mayr *et al.* (2018) noted, it is often difficult to objectively differentiate a foehn using the data from only one surface station.

In this study, to reduce the problems afflicting the previous study by Shibata *et al.* (2010), Japan's south foehns were defined using data from multiple surface stations, as well as upper-level data. Specifically, an event was defined as a foehn when all of the following four conditions were simultaneously satisfied at the Toyama observatory for 2 hr or more:

1. The wind from near-ground level to 900 hPa blew from the mountains (ENE–SSW).
2. Near-ground and 950-hPa wind speeds exceeded 3 and 5 $\text{m}\cdot\text{s}^{-1}$, respectively.
3. The potential temperature was 2 K higher than at the observatories on the Nobi Plain, located in the south-east (Pacific Ocean) side of Honshu.
4. Wind directions changed rapidly, wind speeds increased, and temperatures increased simultaneously, and relative humidity changed near the onset of a foehn.

Conditions (1) and (2) were used to eliminate the cases of land breezes and down-valley winds. These thresholds were determined in consideration of the wind speeds and thicknesses of the thermally induced winds in this area. Condition (3) was used to eliminate warming due to changes in larger scale phenomena, in reference to the methods of Drechsel and Mayr (2008) and Mayr *et al.* (2018). Condition (4) was used to provide conservative estimates, according to expert opinion. This condition was applied for all cases that satisfied conditions (1)–(3). As a result, 198 south foehns were selected between 2006 and 2015. We defined the start of foehns as the time when condition (4) is satisfied and the end of foehns as the time when the wind direction changes to a direction other than from the mountains.

☐

Here, foehns were detected only from high-temperature days to reduce false positives, although such events on other days may have been missed. High-temperature days were defined as follows:

1. The temperature deviation, dT ($24 \text{ hr} \times 365 \text{ days} \times 15 \text{ years}$ of samples), was calculated from the difference between hourly temperature, T ($24 \times 365 \times 15$ samples), and the climate-averaged value of T for each hour and each day, T_C (24×365 samples). In short, $dT = T - T_C$ for each hour and day. Here, T_C was smoothed by the Kolmogorov–Zubenko filter (i.e., the simple moving average of 9 days was repeated three times), according to the JMA method (JMA, 2020).

2. We defined dT_{max} (365 samples) as the daily maximum value of dT .
3. For each month, the top 20% of days with dT_{max} were extracted as the high-temperature days.

2.4 | Classification of synoptic weather patterns

Synoptic weather conditions proximal to the timing of foehn onset were investigated to categorize the synoptic patterns. This task was aimed at improving our understanding of the linkages between foehns and synoptic weather patterns. For our analyses, we employed both subjective, human-made classifications and objective classification via self-organizing mapping (SOM). The reasons for using these two approaches were to retain the benefits of each approach, while also reducing the uncertainty of the results. Subjective analyses involved first classifying historical synoptic weather charts, based on visual analyses, into one of five types: (a) extratropical cyclone over the Sea of Japan, (b) anticyclone, (c) typhoon, (d) stationary front, and (e) others. We then counted the frequency of the foehns appearing in each synoptic weather pattern.

SOM is a kind of neural network that uses unsupervised learning to produce low-dimensional representations (usually in the form of a two-dimensional map) of high-dimensional input vectors (Kohonen, 1982). In climatological studies, the use of SOMs has recently increased and been applied for various purposes, including the recognition of synoptic weather patterns (e.g., Cavazos, 2000; Ohba *et al.*, 2016; Rolinski *et al.*, 2019; Ohba and Sugimoto, 2020). The SOM analytical procedure in this study involved first training the SOM model with the sea level pressure (SLP) data from NCEP (i.e., FNL data proximal to the timing of foehn onset to produce a 3×3 two-dimensional SOM). Here, a total of 496 SLP data points or vectors were used. Each element of the SOM, called a “node,” was initialised with random values and iteratively updated by providing the input SLP vectors. At each iteration, the best-matching unit was selected. The best-matching unit and its neighbouring nodes were then trained to be closer to the input vector. The training process was determined by a learning rate and a “neighbourhood function.” The initial learning rate was 0.1, and it then decreased exponentially. Gaussian was used as the neighbourhood function; this configuration is standard in SOM analyses. We then classified the 198 foehns into 9 SOM node patterns before finally counting the frequency of the foehns corresponding to each SLP pattern obtained from the SOM analysis.

2.5 | Back trajectory analysis and numerical simulations

Back trajectory analysis was performed to understand the typical paths of foehn flow. Prior to trajectory analysis, numerical simulations were conducted with the Weather Research and Forecasting (WRF) model and predictable variables were out every 3 min. Subsequently, the 76 foehn cases that were highly reproducible were selected for back trajectory analysis. A total of 72 parcels were released from 100 m and 500 m above sea level around the Toyama observatory.

The simulation domain of the WRF model is shown in Figure 1b. The horizontal grid spacing was 3 km and the number of vertical layers was 70. Dudhia's simple scheme was used to calculate the shortwave radiation (Dudhia, 1989), the Rapid Radiative Transfer Model (RRTM) was used to calculate the longwave radiation (Mlawer *et al.*, 1997), and the WRF single-moment 6-class cloud microphysics scheme (WSM6) was used to model the physical processes of clouds (Hong *et al.*, 2004). Additionally, the Yonsei University (YSU) scheme was employed to account for boundary layer turbulence (Hong *et al.*, 2006), and the Noah-land surface model (Noah-LSM) was used for ground surface processes (Chen and Dudhia, 2001). The topographical and land use data used in the simulation were created from the National Land Numerical Information data of Japan (Ministry of Land, Infrastructure, Transport and Tourism, 2020). The initial and boundary conditions were created from the NCEP-FNL data.

3 | RESULTS AND DISCUSSION

3.1 | Characteristic synoptic weather patterns

Does Japan's south foehn really only blow while cyclones or typhoons are approaching? We sought to answer this question by reviewing weather charts from the onsets of 198 past foehns between 2006 and 2015. Figure 4 illustrates four types of typical weather charts. Here, the extratropical cyclone-type pattern was defined as the chart type when a cyclone was passing through the Sea of Japan and the Hokuriku region was under the influence of the cyclone. In the typical case, the Hokuriku region was covered by warm-sector air (Figure 4a). The tropical typhoon-type was defined as the chart type when a typhoon was approaching Japan and the Hokuriku region was affected by the advection of warm and moist air from the south (Figure 4b). The anticyclone-type was defined as the

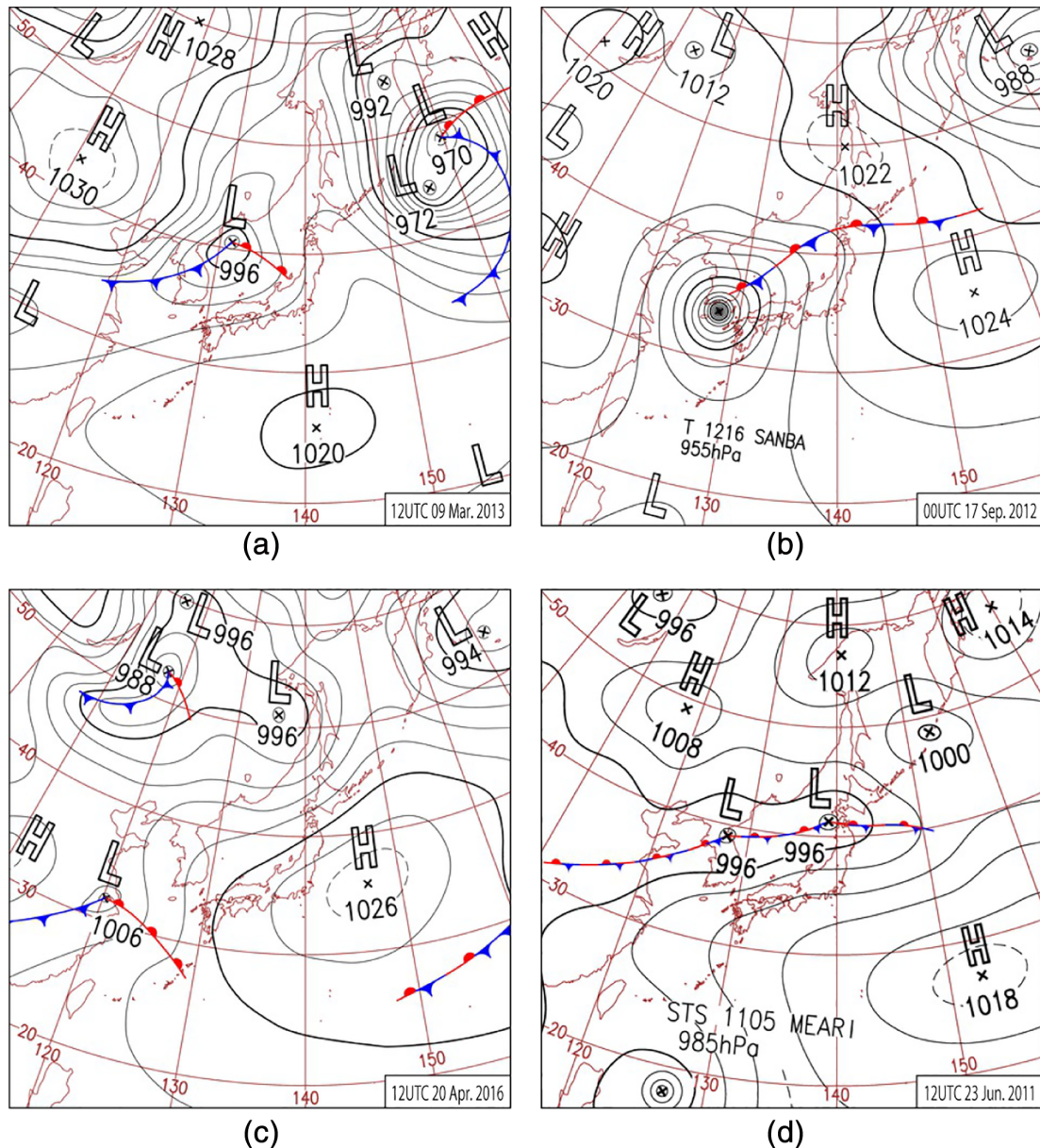


FIGURE 4 Example synoptic weather charts during foehns: (a) extratropical cyclone; (b) typhoon; (c) anticyclone; (d) stationary front [Colour figure can be viewed at wileyonlinelibrary.com]

Extratropical cyclone case	South foehns w/o precipitation	South foehns w/ precipitation in the trajectory	Total
Extratropical cyclone	106	29	135 (68.2%)
Anticyclone	39	0	39 (19.7%)
Typhoon	6	4	10 (5.1%)
Other (e.g., Baiu front, etc.)	9	5	14 (7.1%)
Total	160 (80.8%)	38 (19.2%)	198 (100%)

TABLE 1 Subjective classification of Japan's south foehns+

chart type when an anticyclone was centred on the Pacific Ocean side of the Honshu and the Hokuriku region was under the influence of the anticyclone

(Figure 4c). The stationary front-type was defined the chart type in which a stationary front existed near Japan (Figure 4d).

Table 1 summarizes the frequency with which each weather chart pattern (synoptic pattern) appeared near the time of foehn onset between 2006 and 2015. This table also contains information about the type of foehns. Of the weather charts proximal to foehn onset, the most frequent synoptic pattern was that of an extratropical cyclone. The total number of this type pattern was 135 and accounted for 68.2% of all foehns. This result agrees well with the expectations of many weather forecasters and researchers (e.g., Yoshino, 1975; Nitta and Tatehira, 2000). The second most common synoptic pattern was the anticyclone-type. The total number of this type was 39 and accounted for 19.7% of all foehns. This

finding resulted from carefully analysing weather maps for many foehn cases in this study. The third most common pattern was the typhoon-type, for which there were 10 events, accounting for 5.1% of the total. It is noteworthy that hazardous foehns, which satisfy the 95th percentile of the daily maximum temperature, were all associated with typhoon-type weather patterns.

Until this study, it was thought that Japan's south foehn in the Hokuriku region only occurred under the influence of extratropical cyclones or typhoons. However, the result of our analyses reveals that the south foehn blows even under the control of anticyclones, with a relative frequency of $\sim 1/3$ that of the extratropical cyclone-

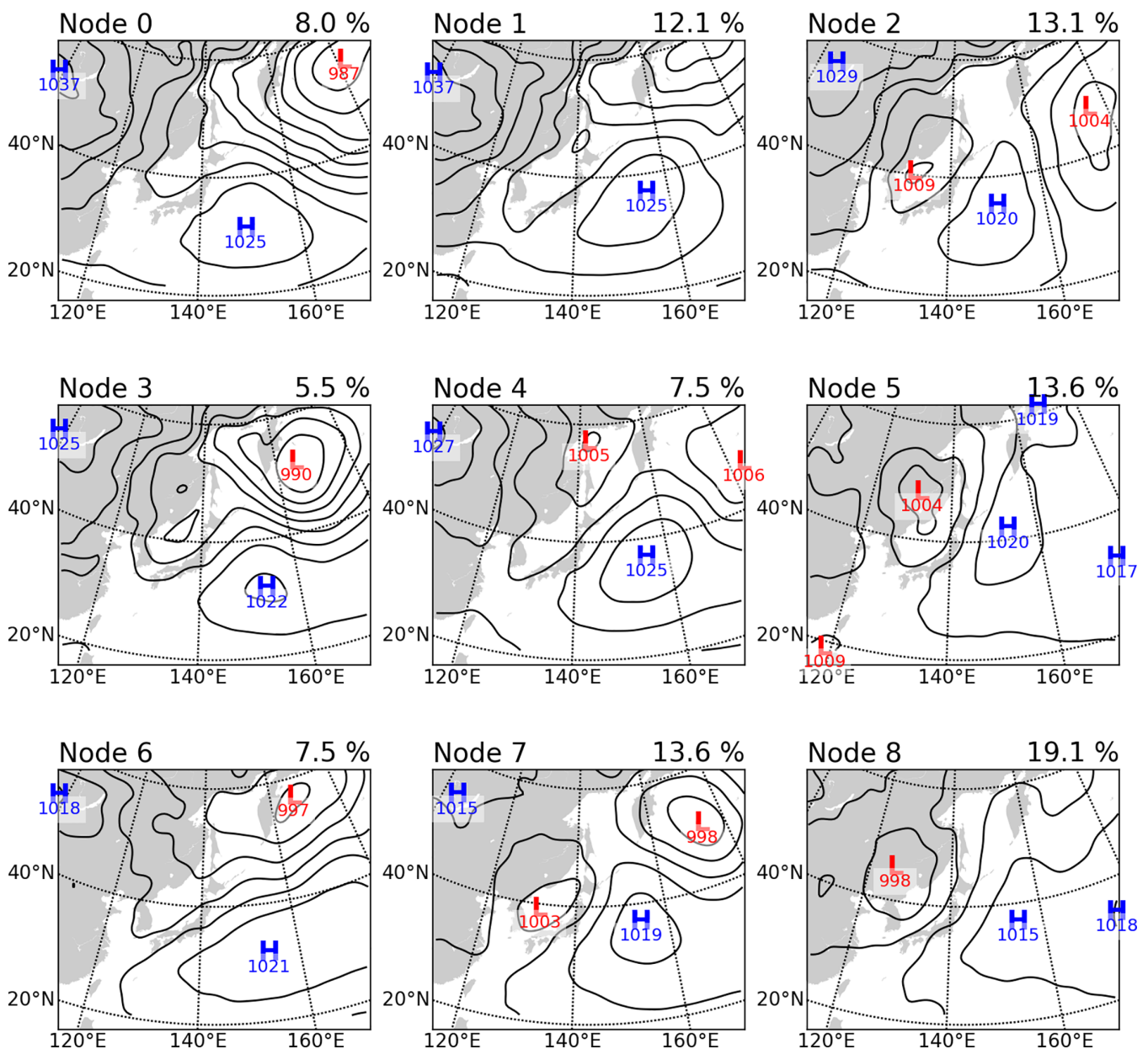


FIGURE 5 Self-organized maps of nodes 0–8. Maps indicate the sea level pressure patterns proximal to the timing of foehn onset (contour intervals of 4 hPa) [Colour figure can be viewed at wileyonlinelibrary.com]

type and nearly four times that of the typhoon-type. Some researchers have suggested that the extratropical cyclone and anticyclone foehn types are the same, and thus there is no reason to distinguish them. In answer to the veracity of this claim, this study confirmed the existence of a discrete anticyclone-type pattern via SOM techniques.

Figure 5 illustrates the nine synoptic weather patterns generated via SOM analysis. In the SOMs, close patterns are allocated into close nodes, and vice versa. Nodes 2 and 7 show typical extratropical cyclone-type patterns, as do Node 5 and Node 8. Indeed, Nodes 2, 5, 7, and 8 are allocated close to each other in the SOM map. In contrast, in Node 0, the entire Hokuriku region and Backbone Mountain appear to lie under the high-pressure system extending over the West Pacific. Thus, this node, which is distinct from Nodes of the extratropical cyclone-type, can be recognized as anticyclonic. The results from the objective pattern analysis via SOM supported those achieved via subjective analysis, wherein there were also anticyclonic synoptic weather patterns observed in the blowing of this wind.

3.2 | Seasonal and hourly frequencies and intensities of foehns

Figure 6a shows the distribution of the monthly frequency for the 198 south foehns between 2006 and 2015. Seasonally, the south foehn most frequently occurred in spring. The frequencies of occurrence in March, April, and May accounted for 11.9, 13.2, and 11.7% of all occurrences, respectively. As is well-known, extratropical cyclones and anticyclones frequently pass over Japan in spring. Extratropical cyclones often produce strong north–south pressure gradients across Japan's Backbone Mountain and southerly winds in the warm sector (Figure 4a). Anticyclones in the Pacific Ocean also produce north–south pressure gradients. The other noteworthy seasonal feature of the south foehn is its relatively low frequency in June. One reason for this is that the Baiu Front stays over Japan from June to mid-July (e.g., Ninomiya and Akiyama, 1992; Tomita *et al.*, 2011).

Figure 6b shows the duration of the south foehn. Most south foehns continue to blow for 5–24 hr. The onset of Japan's south foehns mainly occurs when the Hokuriku region is in the warm sector of an extratropical cyclone and the direction of the wind approaching from the Backbone Mountain range changes to the south. Then, the foehn ends just after the cold front passes over the Hokuriku region. Thus, its resulting duration is reasonable. However, it is also noteworthy that foehn warming is sometimes stopped due to local effects, such as sea breezes.

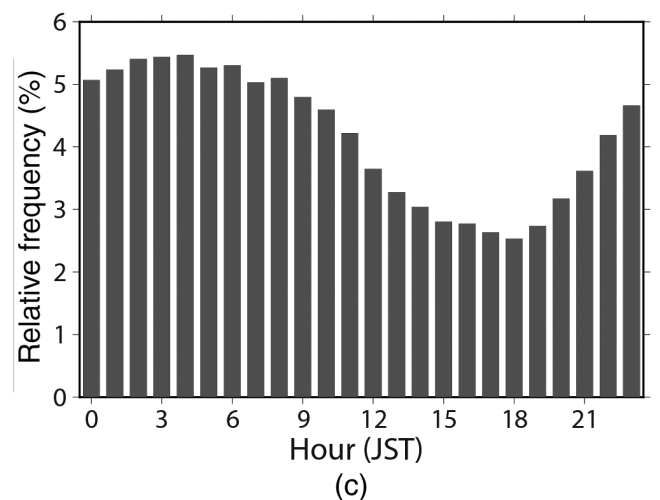
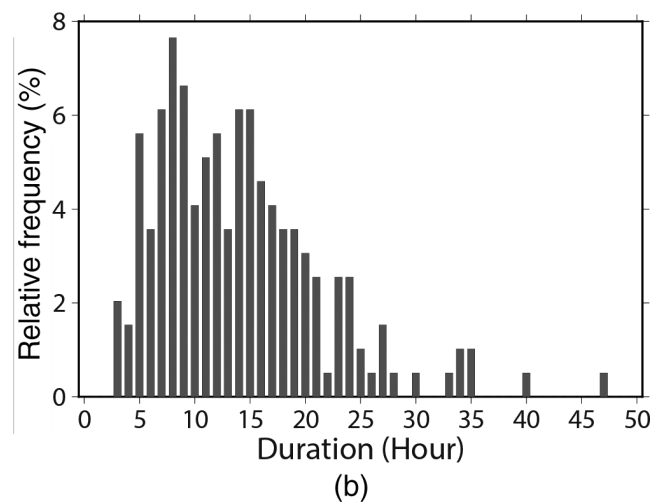
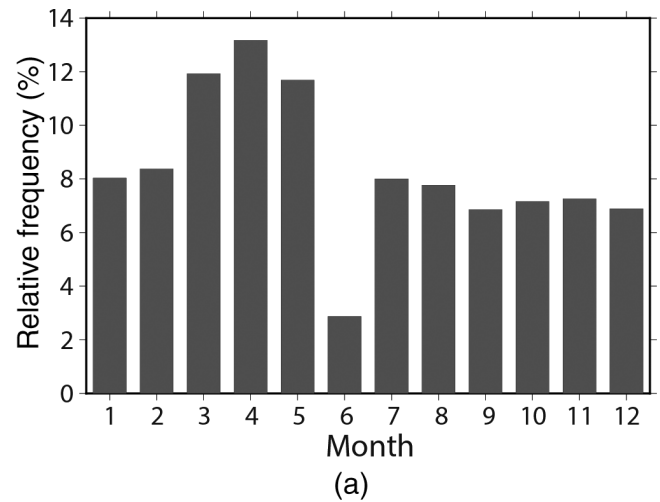


FIGURE 6 Relative frequencies and durations of Japan's south foehns on the Toyama Plain: (a) monthly; (b) duration; (c) hourly. Grey bars of (a) indicate the data collected at the foehn onsets. Grey bars of (b) and (c) indicate the data collected during foehns

Figure 6c shows the clear diurnal variation in foehn activity. The modal onsets and end times of south foehns are 22:00 Japan Standard Time (JST) and 11:00 JST, respectively (Figure 7). The results show that the south

foehn occurs more often during the night and less often in the day. This tendency is particularly found in anticyclone-type foehns (Table 2). One reason for this is that strong winds remove the cold air layer at night when the foehn begins, while another cause may be the influence of thermally driven local circulation. The Toyama Plain faces Toyama Bay on its north side and is adjacent to the Hida Highlands on its south side (Figure 1b). Therefore, sea breezes and up-valley winds can blow during the day and land breezes and down-valley winds can blow at night. Minimally, a local pressure gradient can be generated in a given direction to blow these winds, and such winds or local pressure gradients may break or terminate foehn winds.

Another important aspect of foehn behaviour is the intensity. In this study, we used the potential temperature difference between the Toyama observatory and windward surface stations ($\Delta\theta$) in order to assess the thermal behaviour (Figure 8a). At the time when foehn intensity was the strongest, the mean potential temperature difference between the station on the Toyama Plain and Nobi Plain, $\Delta\theta$ was 6.9 K. This result did not depend on the synoptic pattern (Table 2). The actual intensity of the south foehn could be stronger than the result shown in the figure because the annual mean temperature at Toyama is climatologically 1.4 K lower than the windward site. Similarly, the monthly mean temperature in April when the foehn occurs the most frequently is 1.9 K lower at Toyama than the windward site. South foehns, which bring high temperatures over 35°C to Toyama City, were typhoon-type foehns. It can be said that typhoon-type foehns are more likely to bring dangerously high temperatures than other types. These high temperatures are likely to be influenced not only by the foehn, but also by the advection of warm air from the typhoon.

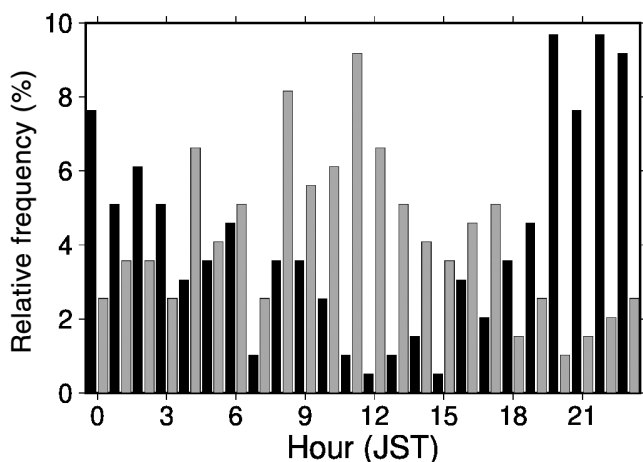


FIGURE 7 Relative frequencies of the onset (black bars) and end (grey bars) times of Japan's south foehns on the Toyama Plain

When examining foehn intensity, the wind speed must also be considered (Figure 8b). The mean wind speed at the time of strongest foehn intensity was 8.5 m s⁻¹. For the very high-wind-speed cases (90th percentile), wind speeds were >11.9 m s⁻¹. This distribution did not depend on the synoptic weather pattern (Table 2). Wind speeds of typhoon-type foehns were not as high as those in the centres of the typhoons because the typhoons were located far from the Hokuriku region when the foehns occurred.

3.3 | Contribution of thermodynamically controlled foehns

Which is the primary type of the south foehn, dynamical, thermodynamical, or multiple? To answer this question, all 198 foehn cases were first classified into those with precipitation on the windward slopes of the mountains and those without. Surprisingly, most of the foehns (80.8%) occurred without precipitation (Table 1). This type accounted for 78.5% of all of the foehns associated with extratropical cyclones, and 60.0% for those associated with typhoons. All the foehns (i.e., 100%) associated with anticyclones were recognized as this type. These results indicate that the more famous thermodynamical mechanism, at least in the case of the south foehn in Japan, does not govern primarily, but rather the dynamical mechanism predominates (Figure 9).

As Takane *et al.* (2015) and Miltenberger *et al.* (2016) noted, not all air parcels are affected by thermodynamical processes, even if they pass through over windward precipitation areas. Therefore, in some of the precipitation cases, foehn warming is due to multiple processes with both dynamical and thermodynamical effects (Figure 9b) and it cannot be conclusively determined that the primary warming process was thermodynamical in nature. In order to identify foehn types with precipitation on windward mountain slopes, we used the results of the back trajectory analysis to examine the height of individual air parcels when the parcels reached over the windward plain of the mountain range. Second, we counted the number of respective air parcels higher and lower than 800 m. If most of the parcels (more than 90%) occupy the lower course, this foehn was identified as a pure thermodynamical mechanism type. Otherwise, the foehn was identified as the multiple mechanism type. Such categorisation is based on the following logic: (a) warming driven by the thermodynamical mechanism should occur in cases when parcels ascend from below 800 m level, as orographic lifting. In this case the parcels pass over the Hida Highlands (that plays a role of the pass/saddle of the mountain range) and descend to the

TABLE 2 General climatology of Japan's south foehns

	Primary season (and month)	Primary onset (% night, 18:00–05:00)	Mean duration (hr)	Mean $\Delta\theta$ (K)	Mean U ($\text{m}\cdot\text{s}^{-1}$)
Extratropical cyclone	Spring (April)	71.9%	13.1	7.0	8.9
Anticyclone	Spring (May)	87.2%	17.8	7.1	7.9
Tropical cyclone	Summer and autumn (September)	66.7%	13.2	6.3	7.9
Other (e.g., Baiu front, etc.)	Summer (July)	78.6%	11.3	5.3	6.5

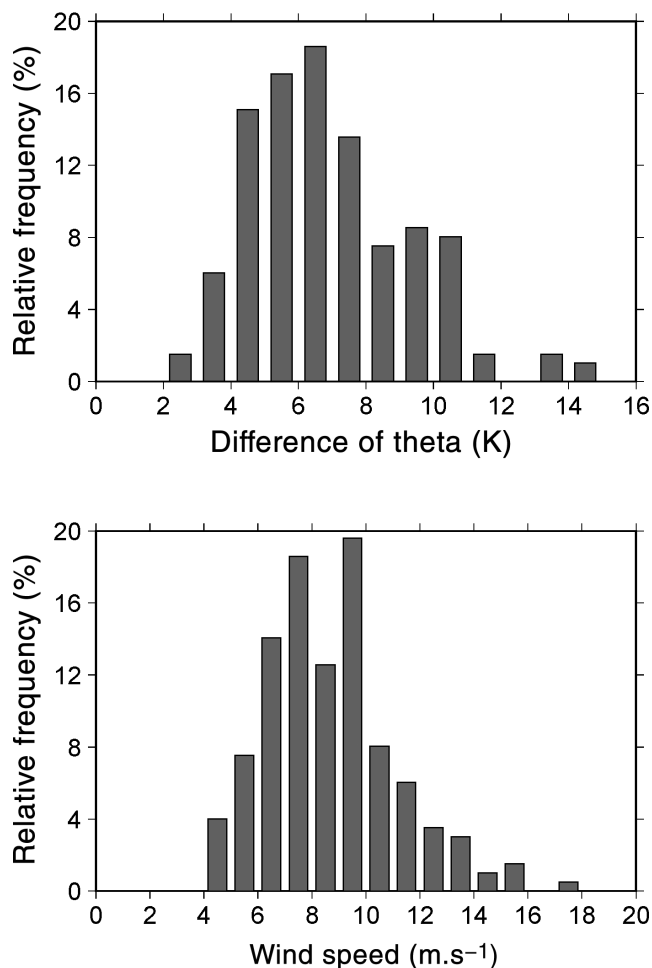


FIGURE 8 Relative frequencies of the intensity of Japan's south foehns. (a) Potential temperature difference between the stations on the Toyama Plain and Nobi Plain. (b) Wind speed at the Toyama observatory. Grey bars indicate the data collected at the times when foehn intensity was the strongest

leeward plain. (b) We set 800 m as the threshold because the lifting condensation level in the windward region was lower than 800 m. Furthermore, 800 m is slightly lower than the elevation of the Hida highlands (about 1,000 m) (Figure 1b). In case of the dynamical foehns without

precipitation on windward mountains slopes, most of the parcels were on courses higher than 800 m in the windward regions.

The results are as follows: of the total 2,736 air parcels of 38 foehn cases with precipitation on windward mountains slopes (72×38 parcels), 68% were high course and 32% were low course (Figure 9). However, simulation at the case level reveals that 30 of 38 cases were predominantly high course and eight cases were predominantly low course. There were only two cases in which more than 90% of the parcels took a low course, which indicates that foehn driven purely by the thermodynamical mechanism may rarely occur.

In this study, the spatial distribution of 9 hr of accumulated precipitation at the time of maximum foehn intensity was generated for 38 foehns with precipitation on windward mountains slopes. After that, precipitation area and precipitation amount were calculated. In all cases, precipitation was observed in the whole area surrounded by the squares shown in Figure A1 in Appendix A. The average 9 hr accumulated precipitation was 13.0 mm (about $1.4 \text{ mm}\cdot\text{hr}^{-1}$). This is comparable to the average precipitation in the foehn cases described by Seibert (1990) identified as dynamical foehns.

These results suggest that foehns with precipitation on windward mountains slopes are not necessarily driven the thermodynamical mechanism, but rather primarily driven by multiple mechanisms.

Focusing on extratropical cyclonic foehns, we analysed the relationship between cyclone location and foehn-type. The location of the cyclone centre differed between foehn types (Figure 10), and there was a tendency for precipitation to occur when cyclones were near Japan, with no precipitation when they were far from Japan. This is reasonable from the viewpoint of a synoptic field. Generally, no precipitation is more likely to occur when Hokuriku is within a warm-sector region of a cyclone, while precipitation is likely to occur when the centre of a cyclone is passing near Hokuriku. To obtain more robust conclusions, more data on foehns with precipitation on windward mountains slopes are needed.

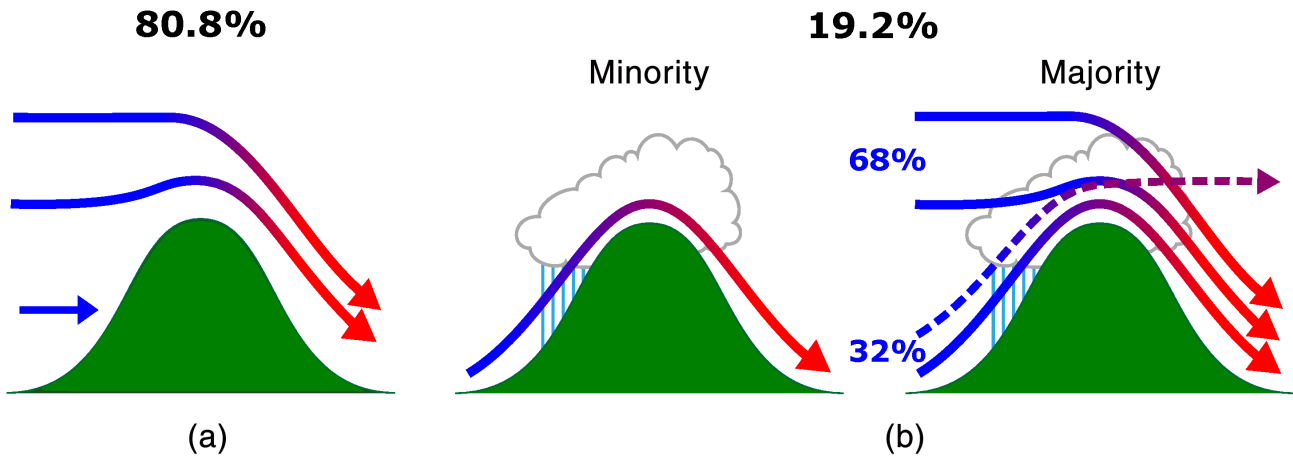


FIGURE 9 Schematic of dynamical, thermodynamical, and multiple mechanism type. Black text indicates the rate of occurrence of each foehn type. Blue text indicates the rate of parcels on higher and lower courses [Colour figure can be viewed at wileyonlinelibrary.com]

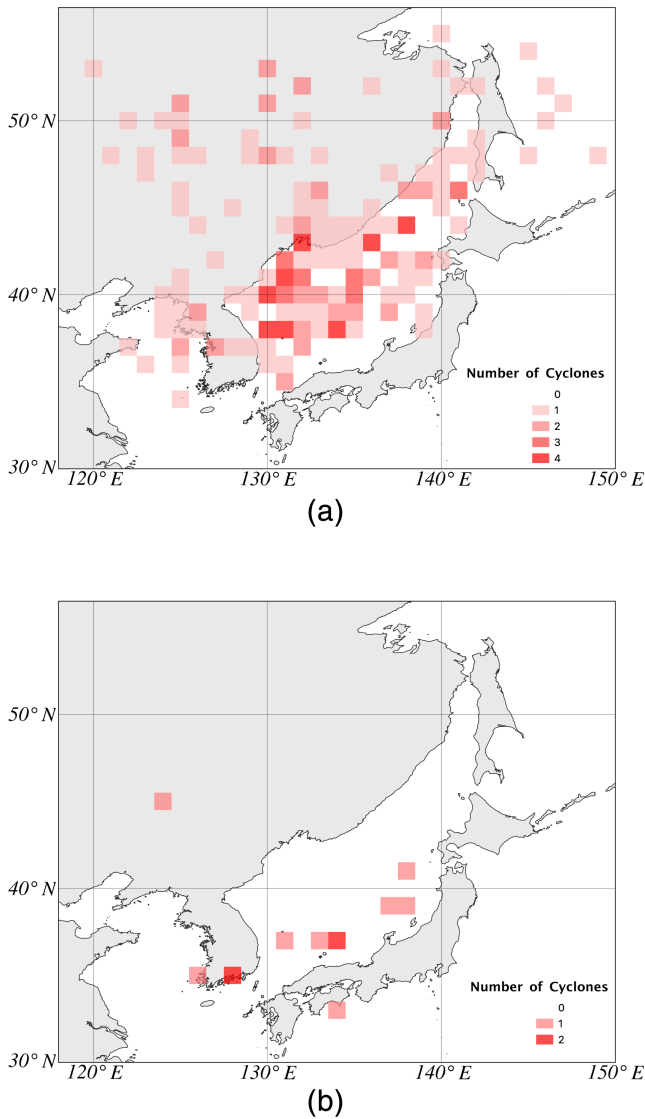


FIGURE 10 Location of the cyclone centres proximal to foehn onset for cyclone-type foehns (a) without precipitation and (b) with precipitation. Colour scales indicate the number of cyclones at each location [Colour figure can be viewed at wileyonlinelibrary.com]

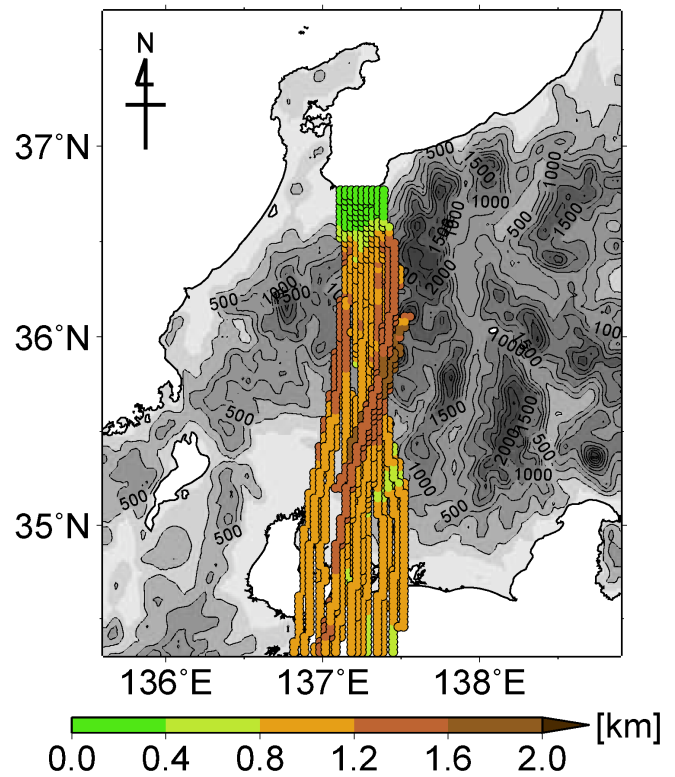


FIGURE 11 Examples of anticyclonic foehn trajectories without precipitation on the windward side. Coloured lines indicate the altitude of the trajectories. Grey scales indicate the topography (contour intervals of 250 m) [Colour figure can be viewed at wileyonlinelibrary.com]

3.4 | Results of back trajectory analysis

The results of back trajectory analyses revealed that the south foehns mainly followed three paths. Most of the anticyclonic foehns with dynamical warming processes (90% for all cases) involved air parcels coming from the south and passing straight over the gap between the Hida

Highlands and Hida Mountains, and then descending from $\sim 1,500$ m (Figure 11). Air parcels did not flow from the bottom of the Hida Highlands; thus, the airflows were not cold-drainage-currents but hybrid of foehn winds and gap winds.

Most of the cyclone-type foehns with dynamical warming process (77% for all cases) exhibited similar

paths as the anticyclone-type foehns (Figure 12a). However, there were two other paths that were observed. One involved air parcels coming from the west hitting the Hida Mountains, turning northward, and then descending from $\sim 1,500$ m (10% for all cases) (Figure 12b). A part of the dynamical effects was the barrier jet. The other pattern observed involved air parcels coming

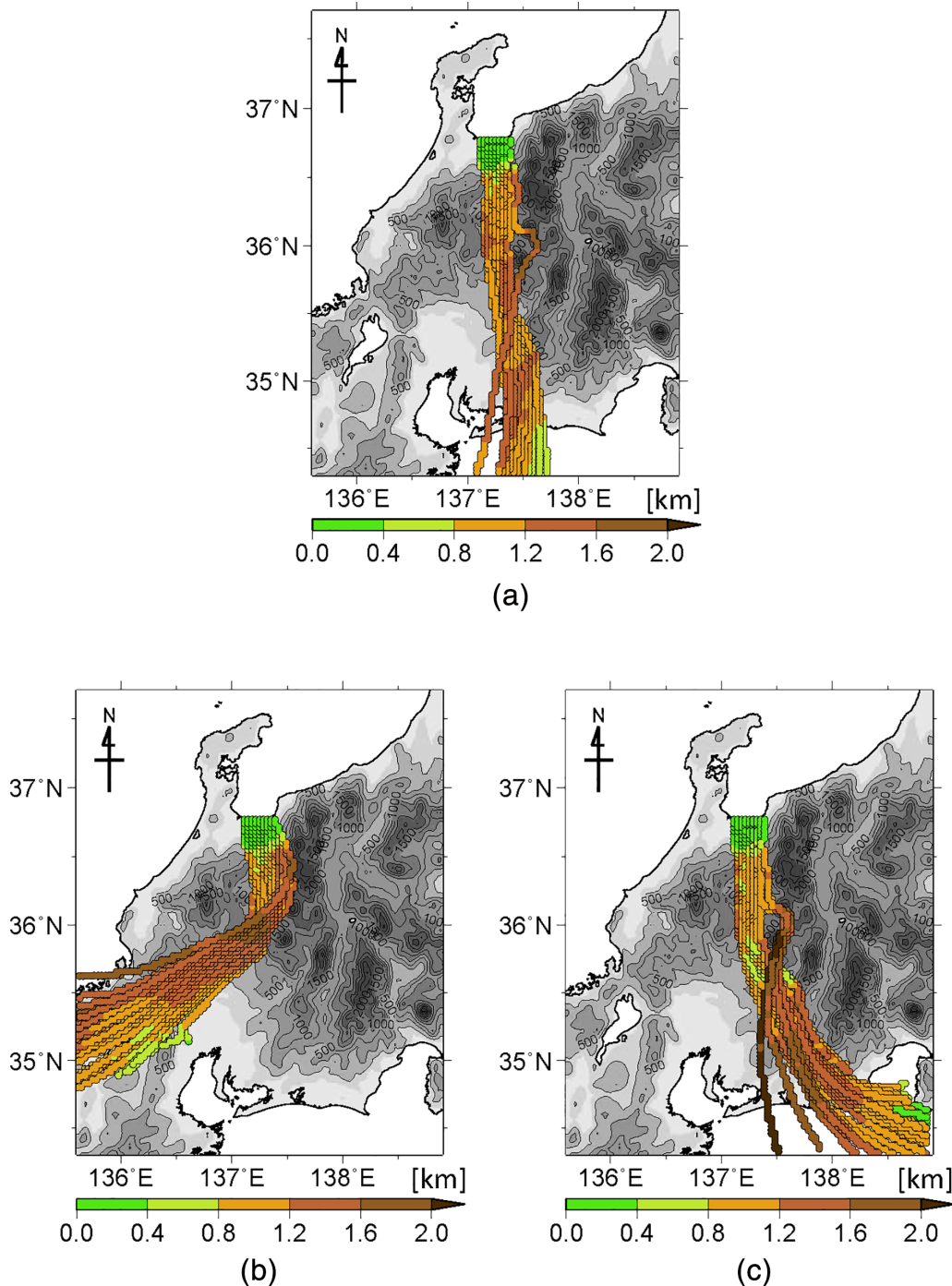
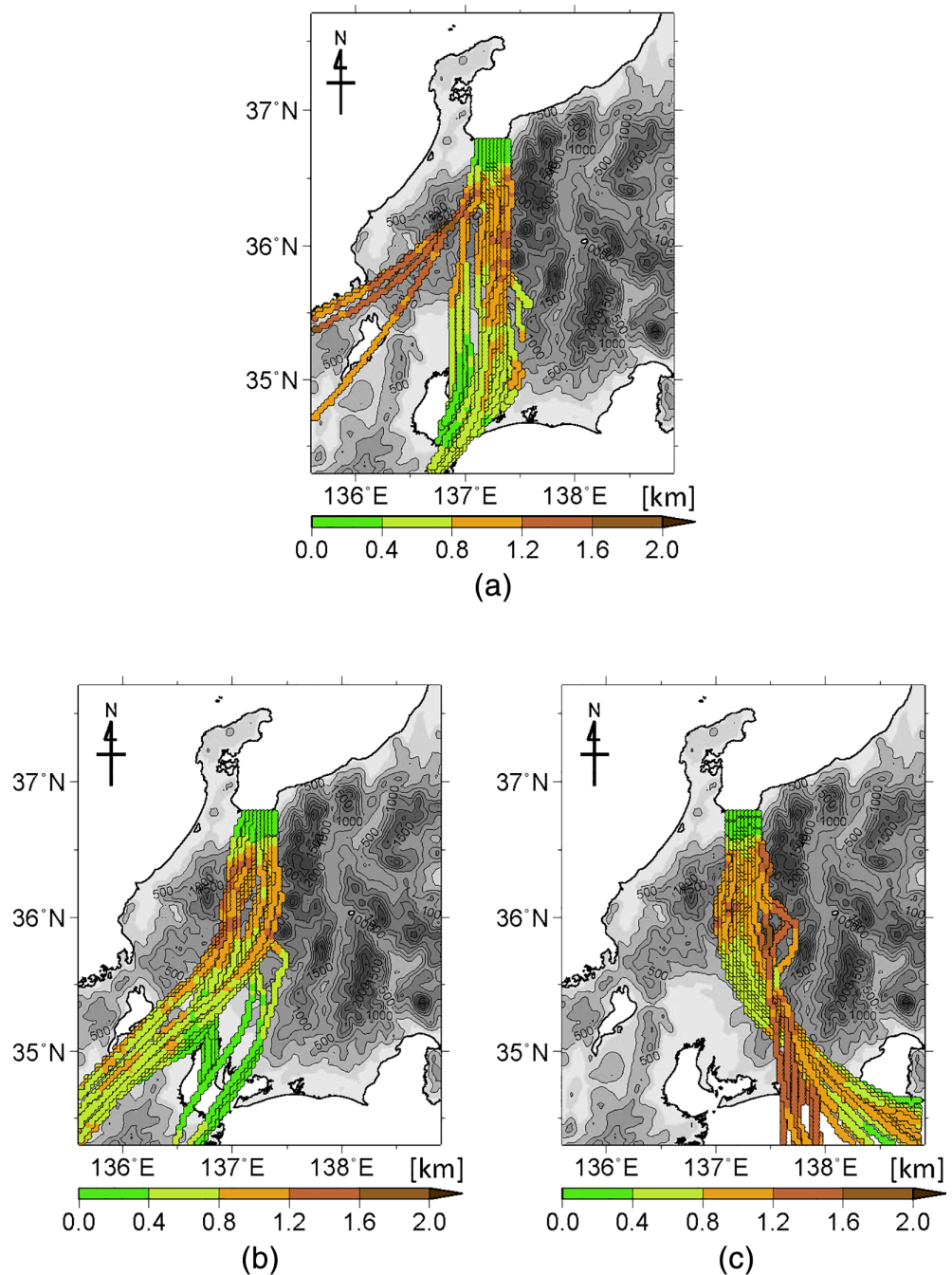


FIGURE 12 Examples of cyclonic foehn trajectories without precipitation on the windward side: (a) south course; (b) west course; (c) east course. Coloured lines indicate the altitude of the trajectories. Grey scales indicate the topography (contour intervals of 250 m) [Colour figure can be viewed at wileyonlinelibrary.com]

FIGURE 13 Examples of cyclonic foehn trajectories with precipitation on the windward side: (a) south course; (b) west course; (c) east course. Coloured lines indicate the altitude of the trajectories. Grey scales indicate the topography (contour intervals of 250 m) [Colour figure can be viewed at wileyonlinelibrary.com]



from the east hitting the Ryohaku Mountains, turning northward, and then descending from 1,500 m (11% for all cases) (Figure 12c). These latter paths were newly recognized in this study. In the cyclonic foehns with precipitation over the windward areas, the courses were similar to those of the cyclonic foehns without precipitation, but some air parcels (32%) experienced uplift on the windward slopes (Figures 9 and 13). The percentages for the south, west, and east course were 66, 18, and 16%, respectively.

3.5 | Comparison with the results of previous studies

We compared the results from this study to those from two previous studies. Shibata *et al.* (2010) and Arakawa *et al.* (1982) stated that Japan's south foehn blows in response to extratropical cyclones and typhoons; however, we found that $\sim 19.7\%$ of all foehns in a 10-year period occurred under the influence of anticyclones. In the commentaries of weather forecasters and textbook

descriptions, foehn warming in Japan has mostly been explained according to the thermodynamical mechanism, but this study revealed that the thermodynamical mechanism could explain at most only 19.2% of the 198 documented foehn warming events between 2006 and 2015. In fact, most of this 19.2% was likely driven by the multiple mechanism rather than the pure thermodynamical mechanism, which was rarely observed. Additionally, the thermodynamical mechanism could not explain foehn warming under the control of anticyclones.

From surface meteorological station data, Arakawa *et al.* (1982) supposed that the foehns blowing on the Toyama Plain are derived from winds on the Nobi Plain, which cross the Hida Highlands and reach Toyama. Ishizaki and Takayabu (2009) simulated this course, and the results of our study strongly support their findings and enhance their robustness by the addition of statistical analyses. We also found that there were two other minor paths for cyclonic foehns. In contrast, the path to reach the Toyama Plain by detouring to the west of the Ibuki and Ryohaku mountains (E and F in Figure 1b), as estimated in a previous study by Ishizaki and Takayabu (2009), was not supported in this study.

We compared Japan's south foehn with foehns in other parts of the world from the diurnal cycle perspective. In the Alps, the Swiss foehns tend to start during the daytime and end at night (Cetti *et al.*, 2015). The Austrian foehns exhibit a diurnal cycle with the lowest probability during nighttime due to cold pool formation in deep valleys (such as the Inn Valley or the Rhine Valley) (Mayr *et al.*, 2007; Haid *et al.*, 2020), but this characteristic is weaker at higher locations closer to the main Alpine crest (such as the Wipp Valley) as cold pool formation is less of a factor (Mayr *et al.*, 2007). On the other hand, chinook winds of northwest America occur most frequently during the nighttime and early morning (Brinkmann, 1974; Whiteman and Whiteman, 1974). Meanwhile, in California, United States, Santa Ana winds tend to blow in the morning (Guzman-Morales *et al.*, 2016). This might be because of a thermally-driven local pressure-gradient force (Hughes and Hall, 2010). Japan's south foehns also tend to start at night and end in the morning due to development of a thermally-driven local pressure gradient and the removal of the nocturnal surface inversion layer.

4 | CONCLUSIONS

The characteristics of Japan's south foehns that blow in the Hokuriku region were revealed in this study, which is the first comprehensive climatological study on foehn warming events in this region. Prior to our analyses,

198 foehns were extracted from the top 20% high-temperature days in 2006–2015. We found that most of Japan's south foehns tend to occur under three synoptic weather conditions: extratropical cyclones in the Sea of Japan (68.2% of all foehns), anticyclones south of Japan (19.7%), and typhoons around Japan (5.1%).

The potential temperature in the foehn area was, on average, 6.9°C higher than on the windward plain. The mean wind speed was 8.5 m·s⁻¹, and most of the hazardous foehns, whose daily maximum temperatures exceeded 35°C, were caused by typhoons. Japan's south foehns are mostly onset at night and end or pause during the day. A possible reason for this behaviour is the removal of the nocturnal stable layer and development of daytime local pressure gradients. South foehns occurred in all of the years sampled and in all months, with a slightly greater number of events in spring.


Diagnostic analysis suggests that the primary mechanism underlying foehn warming is the isentropic draw-down, which is the adiabatic compression of the air due to descent. Surprisingly, the thermodynamical and multiple mechanisms could explain only 19.2% of the all foehn warming events; meanwhile, the results of the backward trajectory revealed that most of these are likely attributed to the multiple mechanism. Hence, occurrence of the south foehn of pure thermodynamical mechanism type is rare. Interestingly, even in the typhoon type, only 40.0% of the foehn warming events associated with the typhoon were induced by the thermodynamical mechanism. Furthermore, back trajectory analyses also showed that most of the air parcels descend from the Hida Highlands between the two mountain ranges, like as hybrid type of foehn winds and gap winds. Combined, these findings provide a holistic view of the mechanisms underlying foehn warming on the Toyama Plain, which may be used to predict the occurrence of dangerously high temperatures and thus, to mitigate the impacts of such extremes on residents and rice crops.

ACKNOWLEDGEMENTS

This work was supported by Cabinet Office, Government of Japan, Cross-ministerial Strategic Innovation Promotion Program (SIP), “Technologies for creating next-generation agriculture, forestry and fisheries” (funding agency: Bio-oriented Technology Research Advancement Institution, NARO). Part of this work is based on results obtained from a project commissioned by the New Energy and Industrial Technology Development Organization (NEDO). Part of this research was performed by the Environment Research and Technology Development Fund JPMEERF20192005 of the Environmental Restoration and Conservation Agency of Japan. We thank Yuma Imai, Shingo Nakamura, Tomoka Maeda, and Miru Maebata for their help in

producing the figures, as well as Hiroki Kobayashi and Ryuhei Kimura for their assistance in confirming the data.

ORCID

Hiroyuki Kusaka  <https://orcid.org/0000-0002-0326-7179>

Quang-Van Doan  <https://orcid.org/0000-0002-2794-5309>

REFERENCES

- Arakawa, S., Yamada, K. and Toya, T. (1982) A study of foehn in the Hokuriku district using the AMeDAS data. *Papers in Meteorology and Geophysics*, 33, 149–163. <https://doi.org/10.2467/mripapers.33.149>.
- Barry, G.R. (2008) *Mountain Weather and Climate*, 3rd edition. Cambridge, MA: Cambridge University Press, p. 506. <https://doi.org/10.1017/CBO9780511754753>.
- Beran, D.W. (1967) Large amplitude lee waves and Chinook winds. *Journal of Applied Meteorology*, 6, 865–877. [https://doi.org/10.1175/1520-0450\(1967\)006<0865:LALWAC>2.0.CO;2](https://doi.org/10.1175/1520-0450(1967)006<0865:LALWAC>2.0.CO;2).
- Brinkmann, W. A. R. (1973) A climatological study of strong downslope winds in the Boulder area. *NCAR Cooperative Thesis No.27/INSTARR Occasional Paper No.7*, University of Colorado, 229 pp.
- Brinkmann, W.A.R. (1974) Strong downslope winds at Boulder, Colorado. *Monthly Weather Review*, 102(8), 592–602. [https://doi.org/10.1175/1520-0493\(1974\)102<0592:SDWABC>2.0.CO;2](https://doi.org/10.1175/1520-0493(1974)102<0592:SDWABC>2.0.CO;2).
- Cavazos, T. (2000) Large-scale circulation anomalies conducive to extreme precipitation events and derivation of daily rainfall in northeastern Mexico and southeastern Texas. *Journal of Climate*, 12(5), 1506–1523. [https://doi.org/10.1175/1520-0442\(1999\)012<1506:LSCACT>2.0.CO;2](https://doi.org/10.1175/1520-0442(1999)012<1506:LSCACT>2.0.CO;2).
- Cetti, C., Buzzi, M. and Sprenger, M. (2015) Climatology of alpine north foehn. *Scientific Reports*, 100, 76.
- Chen, F. and Dudhia, J. (2001) Coupling an advanced land-surface/hydrology model with the Penn State/NCAR MM5 modeling system. Part I: model description and implementation. *Monthly Weather Review*, 129(4), 569–585. [https://doi.org/10.1175/1520-0493\(2001\)129<0569:CAALSH>2.0.CO;2](https://doi.org/10.1175/1520-0493(2001)129<0569:CAALSH>2.0.CO;2).
- Drobinski, P.R., et al. (2007) Foehn in the Rhine valley during MAP: A review of its multiscale dynamics in complex valley geometry. *Quarterly Journal of the Royal Meteorological Society*, 133(625), 897–916. <https://doi.org/10.1002/qj.70>.
- Drechsel, S. and Mayr, G. (2008) Objective forecasting of foehn winds for a subgrid-scale alpine valley. *Weather and Forecasting*, 23(2), 205–218. <https://doi.org/10.1175/2007WAF2006021.1>.
- Dudhia, J. (1989) Numerical study of convection observed during the Winter Monsoon Experiment using a mesoscale two-dimensional model. *Journal of the Atmospheric Sciences*, 46(20), 3077–3107. [https://doi.org/10.1175/1520-0469\(1989\)046<3077:NSOCOD>2.0.CO;2](https://doi.org/10.1175/1520-0469(1989)046<3077:NSOCOD>2.0.CO;2).
- Durrán, D.R. (1986) Another look at downslope windstorms. Part I: the development of analogs to supercritical flow in an infinitely deep, continuously stratified fluid. *Journal of the Atmospheric Sciences*, 43(21), 2527–2543. [https://doi.org/10.1175/1520-0469\(1986\)043<2527:ALADWP>2.0.CO;2](https://doi.org/10.1175/1520-0469(1986)043<2527:ALADWP>2.0.CO;2).
- Elvidge, A.D. and Renfrew, I.A. (2016) The causes of foehn warming in the lee of mountains. *Bulletin of the American Meteorological Society*, 97(3), 455–466. <https://doi.org/10.1175/BAMS-D-1400194.1>.
- Elvidge, A.D., Renfrew, I.A., King, J.C., Orr, A. and Lachlan-Cope, T.A. (2016) Foehn warming distributions in non-linear and linear flow regimes: A focus on the Antarctic Peninsula. *Quarterly Journal of the Royal Meteorological Society*, 142(695), 618–631. <https://doi.org/10.1002/qj.2489>.
- Elvidge, A.D., Munneke, P.K., King, J.C., Renfrew, I.A. and Gilbert, E. (2020) Atmospheric drivers of melt on Larsen C ice shelf: surface energy budget regimes and the impact of foehn. *Journal of Geophysical Research. Atmospheres*, 125(17), e2020JD032463. <https://doi.org/10.1029/2020JD032463>.
- Gohm, A. and Mayr, G.J. (2004) Hydraulic aspects of föhn winds in an alpine valley. *Quarterly Journal of the Royal Meteorological Society*, 130(597), 449–480. <https://doi.org/10.1256/qj.03.28>.
- Guzman-Morales, J., Gershunov, A., Theiss, J., Li, H. and Cayan, D. (2016) Santa Ana winds of Southern California: their climatology, extremes, and behavior spanning six and a half decades. *Geophysical Research Letters*, 43(6), 2827–2834. <https://doi.org/10.1002/2016GL067887>.
- Haid, M., Gohm, A., Umek, L., Ward, H.C., Muschinski, T., Lehner, L. and Rotach, M.W. (2020) Foehn-cold pool interactions in the Inn Valley during PIANO IOP2. *Quarterly Journal of the Royal Meteorological Society*, 146(728), 1232–1263. <https://doi.org/10.1002/qj.3735>.
- Hann, J. (1866) Zur Frage u'ber den Ursprung des Fo'hns. *Zeitschrift der Österreichischen Gesellschaft für Meteorologie*, 1, 257–263.
- Hoinka, K.P. (1985a) What is a foehn clearance? *Bulletin of the American Meteorological Society*, 66(9), 1123–1132. [https://doi.org/10.1175/1520-0477\(1985\)066<1123:WIAFC>2.0.CO;2](https://doi.org/10.1175/1520-0477(1985)066<1123:WIAFC>2.0.CO;2).
- Hoinka, K.P. (1985b) Observation of the airflow over the alps during a foehn event. *Quarterly Journal of the Royal Meteorological Society*, 111, 199–224. <https://doi.org/10.1002/qj.49711146709>.
- Hong, S.Y., Dudhia, J. and Chen, S.H. (2004) A revised approach to ice microphysical processes for the bulk parameterization of clouds and precipitation. *Monthly Weather Review*, 132(1), 103–120. [https://doi.org/10.1175/1520-0493\(2004\)132<0103:ARATIM>2.0.CO;2](https://doi.org/10.1175/1520-0493(2004)132<0103:ARATIM>2.0.CO;2).
- Hong, S.Y., Noh, Y. and Dudhia, J. (2006) A new vertical diffusion package with an explicit treatment of entrainment processes. *Monthly Weather Review*, 134(9), 2318–2341. <https://doi.org/10.1175/MWR3199.1>.
- Hughes, M. and Hall, A. (2010) Local and synoptic mechanisms causing Southern California's Santa Ana winds. *Climate Dynamics*, 34, 847–857. <https://doi.org/10.1007/s00382-009-0650-4>.
- Ishizaki, N. and Takayabu, I. (2009) On the warming events over Toyama Plain by using NHRCM. *SOLA*, 5, 129–132. <https://doi.org/10.2151/sola.2009-033>.
- Japan Meteorological Agency (2020) Explanation of meteorological observation statistics. https://www.data.jma.go.jp/obd/stats/data/kaisetu/shishin/shishin_all.pdf (in Japanese).
- Jaubert, G., Bougeault, P., Berger, H., Chimani, B., Flamant, C., Häberli, C., Lothon, M., Nuret, M. and Vogt, S. (2005) Numerical simulation of meso-gamma scale features of föhn at ground level in the Rhine valley. *Quarterly Journal of the Royal Meteorological Society*, 131(608), 1339–1361. <https://doi.org/10.1256/qj.03.197>.

- Kohonen, T. (1982) Self-organized formation of topologically correct feature maps. *Biological Cybernetics*, 43, 59–69. <https://doi.org/10.1007/BF00337288>.
- Koyanagi, T. and Kusaka, H. (2019) A climatological study of the strongest local winds of Japan “Inami-kaze”. *International Journal of Climatology*, 40(2), 1007–1021. <https://doi.org/10.1002/joc.6252>.
- Kusaka, H. and Fudeyasu, H. (2017) Review of downslope windstorms in Japan. *Wind and Structures*, 24(6), 637–656. <https://doi.org/10.12989/was.2017.24.6.637>.
- Lilly, D.K. (1978) A severe downslope windstorm and aircraft turbulence event induced by a mountain wave. *Journal of the Atmospheric Sciences*, 35(1), 59–77. [https://doi.org/10.1175/1520-0469\(1978\)035<0059:ASDWAA>2.0.CO;2](https://doi.org/10.1175/1520-0469(1978)035<0059:ASDWAA>2.0.CO;2).
- Mayr, G.J., Armi, L., Gohm, A., Zängl, G., Durran, D.R., Flamant, C., Gaberšek, S., Mobbs, S., Ross, A. and Weissmann, M. (2007) Gap flows: results from the Mesoscale Alpine Programme. *Quarterly Journal of the Royal Meteorological Society*, 133(625), 881–896. <https://doi.org/10.1002/qj.66>.
- Mayr, G.J., Plavcan, D., Armi, L., Elvidge, A., Grisogono, B., Horvath, K., Jackson, P., Neururer, A., Seibert, P., Steenburgh, J.W., Stiperski, I., Sturman, A., Vecenaj, Z., Vergeiner, J., Vosper, S. and Zängl, G. (2018) The community foehn classification experiment. *Bulletin of the American Meteorological Society*, 99(11), 2229–2235. <https://doi.org/10.1175/BAMS-D-17-0200.1>.
- McGowan, H.A. and Sturman, A.P. (1996) Regional and local scale characteristics of foehn wind events over the South Island of New Zealand. *Meteorology and Atmospheric Physics*, 58, 151–164. <https://doi.org/10.1007/BF01027562>.
- McGowan, H.A., Sturman, A.P., Kossmann, M. and Zawar-Reza, P. (2002) Observations of foehn onset in the southern Alps, New Zealand. *Meteorology and Atmospheric Physics*, 79, 215–230. <https://doi.org/10.1007/s007030200004>.
- Miltenberger, A.K., Reynolds, S. and Sprenger, M. (2016) Revisiting the latent heating contribution to foehn warming: Lagrangian analysis of two foehn events over the Swiss Alps. *Quarterly Journal of the Royal Meteorological Society*, 142(698), 2194–2204. <https://doi.org/10.1002/qj.2816>.
- Ministry of Land, Infrastructure, Transport and Tourism (2020) <https://nlftp.mlit.go.jp/ksj/> (in Japanese)
- Mlawer, E.J., Taubman, S., Brown, J., Iacono, P.D. and Clough, S.A. (1997) Radiative transfer for inhomogeneous atmospheres: RRTM, a validated correlated- k model for the longwave. *Journal of Geophysical Research*, 102(D14), 16663–16682. <https://doi.org/10.1029/97JD00237>.
- Mori, K. and Sato, T. (2014) Spatio-temporal variation of high-temperature events in Hokkaido, North Japan. *Journal of the Meteorological Society of Japan*, 92(4), 327–346. <https://doi.org/10.2151/jmsj.2014-404>.
- Muramatsu, K. (1976) The occurrence and damage to paddy-field rice by foehn in the Hokuriku district, Japan. *Bulletin of the Hokuriku Agricultural Experiment Station*, 19, 25–43 (in Japanese with English Abstract).
- Ninomiya, K. and Akiyama, T. (1992) Multi-scale features of Baiu, the summer monsoon over Japan and the East Asia. *Journal of the Meteorological Society of Japan*, 70(1B), 467–495. https://doi.org/10.2151/jmsj1965.70.1B_467.
- Nishi, A. and Kusaka, H. (2019) Effect of foehn wind on record-breaking high temperature event (41.1 degrees C) at Kumagaya on 23 July 2018. *SOLA*, 15, 17–21. <https://doi.org/10.2151/sola.2019-004>.
- Nishi, A., Kusaka, H., Vitanova, L.L. and Imai, Y. (2019) Contributions of foehn and urban heat Island to the extreme high-temperature event in Niigata city during the night of 23–24 August 2018. *SOLA*, 15, 132–136. <https://doi.org/10.2151/sola.2019-024>.
- Nitta, T. and Tatehira, R. (2000) *Techniques of the Weather Forecasting: For the Weather Forecasters*. Tokyo: Tokyo-do Press, p. 343 (in Japanese).
- Ohba, M., Nohara, D. and Kadokura, S. (2016) Impacts of synoptic circulation patterns on wind power ramp events in East Japan. *Renewable Energy*, 96, 591–602. <https://doi.org/10.1016/j.renene.2016.05.032>.
- Ohba, M. and Sugimoto, S. (2020) Impacts of climate change on heavy wet snowfall in Japan. *Climate Dynamics*, 54, 3151–3164. <https://doi.org/10.1007/s00382-020-05163-z>.
- Orr, A., Marshall, G.J., Hunt, J.C., Sommeria, J., Wang, C.G., Van Lipzig, N.P., Cresswell, D. and King, J.C. (2008) Characteristics of summer airflow over the Antarctic Peninsula in response to recent strengthening of westerly circumpolar winds. *Journal of the Atmospheric Sciences*, 65(4), 1396–1413. <https://doi.org/10.1175/2007JAS2498.1>.
- Raphael, M.N. (2003) The Santa Ana winds of California. *Earth Interactions*, 7(8), 1–13. [https://doi.org/10.1175/1087-3562\(2003\)007<0001:TSAWOC>2.0.CO;2](https://doi.org/10.1175/1087-3562(2003)007<0001:TSAWOC>2.0.CO;2).
- Richiner, H. and Hächler, P. (2013) Understanding and forecasting Alpine foehn. In: Chow, F.K., De Wekker, S.F.J. and Snyder, B. J. (Eds.) *Mountain Weather Research and Forecasting*. Dordrecht: Springer, pp. 219–260. https://doi.org/10.1007/978-94-007-4098-3_4.
- Rolinski, T., Capps, S.B. and Zhuang, W. (2019) Santa Ana winds: A descriptive climatology. *Weather and Forecasting*, 34(2), 257–275. <https://doi.org/10.1175/WAF-D-18-0160.1>.
- Saito, K. and Ikawa, M. (1993) A numerical study of the local downslope wind “Yamaji-kaze” in Japan. Part 2: non-linear aspect of the 3-D flow over a mountain range with a col. *Journal of the Meteorological Society of Japan*, 69(1), 31–56. https://doi.org/10.2151/jmsj1965.69.1_31.
- Saito, K. (1994) A numerical study of the local downslope wind “Yamaji-kaze” in Japan. part 3: numerical simulation of the 27 September 1991 windstorm with a non-hydrostatic multi-nested model. *Journal of the Meteorological Society of Japan*, 72(2), 301–329. https://doi.org/10.2151/jmsj1965.72.2_301.
- Saito, K., Fujita, T., Yamada, Y., Ishida, J., Kumagai, Y., Aranami, K., Ohmori, S., Nagasawa, R., Kumagai, S., Muroi, C., Kato, T., Eito, H. and Yamazaki, Y. (2006) The operational JMA non-hydrostatic mesoscale model. *Monthly Weather Review*, 134(4), 1266–1297. <https://doi.org/10.1175/MWR3120.1>.
- Seibert, P. (1990) South foehn studies since the ALPEx experiment. *Meteorology and Atmospheric Physics*, 43, 91–103. <https://doi.org/10.1007/BF01028112>.
- Shibata, Y., Kawamura, R. and Hatsushika, H. (2010) Role of large-scale circulation in triggering foehns in the Hokuriku district of Japan during midsummer. *Journal of the Meteorological Society of Japan*, 88(3), 313–324. <https://doi.org/10.2151/jmsj.2010-304>.
- Takane, Y. and Kusaka, H. (2011) Formation mechanisms of the extreme high surface air temperature of 40.9°C, observed in the

- Tokyo metropolitan area: considerations of dynamic foehn and foehnlike wind. *Journal of Applied Meteorology and Climatology*, 50(9), 1827–1841. <https://doi.org/10.1175/JAMC-D-10-05032.1>.
- Takane, Y., Kusaka, H. and Kondo, H. (2015) Investigation of a recent extreme high-temperature event in the Tokyo metropolitan area using numerical simulations: the potential role of a 'hybrid' foehn wind. *Quarterly Journal of the Royal Meteorological Society*, 141(690), 1857–1869. <https://doi.org/10.1002/qj.2490>.
- Tomita, T., Yamaura, T. and Hashimoto, T. (2011) Interannual variability of the Baiu season near Japan evaluated from the equivalent potential temperature. *Journal of the Meteorological Society of Japan*, 89(5), 517–537. <https://doi.org/10.2151/jmsj.2011-507>.
- Turton, J.V., Kirchgassner, A., Ross, A.N. and King, J.C. (2018) The spatial distribution and temporal variability of föhn winds over the Larsen C ice shelf, Antarctica. *Quarterly Journal of the Royal Meteorological Society*, 144(713), 1169–1178. <https://doi.org/10.1002/qj.3284>.
- Wada, H., Nonami, H., Yabuoshi, Y., Maruyama, A., Tanaka, A., Wakamatsu, K., Sumi, T., Wakiyama, Y., Ohuchida, M. and Morita, S. (2011) Increased ring-shaped chalkiness and osmotic adjustment when growing rice grains under foehn-induced dry wind condition. *Crop Science*, 51(4), 1703–1715. <https://doi.org/10.2135/cropsci2010.08.0503>.
- Whiteman, C. D. and Whiteman, J. G. (1974) An historical climatology of damaging downslope windstorms at Boulder, Colorado. *NOAA Technical Report*, ERL 336-APCL 35. pp. 62.
- Würsch, M. and Sprenger, M. (2015) Swiss and Austrian Foehn revisited: A Lagrangian-based analysis. *Meteorologische Zeitschrift*, 24(3), 225–242. <https://doi.org/10.1127/metz/2015/0647>.
- Yoshino, M. (1975) *Climate in a Small Area—An Introduction to Local Meteorology*. Tokyo: University of Tokyo Press, p. 549.
- Zängl, G. (2003) Deep and shallow south foehn in the region of Innsbruck: typical features and semi-idealized numerical simulations. *Meteorology and Atmospheric Physics*, 83, 237–262. <https://doi.org/10.1007/s00703-002-0565-7>.
- Zängl, G. (2004) Numerical simulations of the foehn in the Rhine valley on October 24, 1999 (MAP IOP 10). *Monthly Weather Review*, 132(1), 368–389. [https://doi.org/10.1175/1520-0493\(2004\)132<0368:NSOTFI>2.0.CO;2](https://doi.org/10.1175/1520-0493(2004)132<0368:NSOTFI>2.0.CO;2).

How to cite this article: Kusaka H, Nishi A, Kakinuma A, Doan Q-V, Onodera T, Endo S. Japan's south foehn on the Toyama Plain: Dynamical or thermodynamical mechanisms? *Int J Climatol*. 2021;41:5350–5367. <https://doi.org/10.1002/joc.7133>

APPENDIX A.

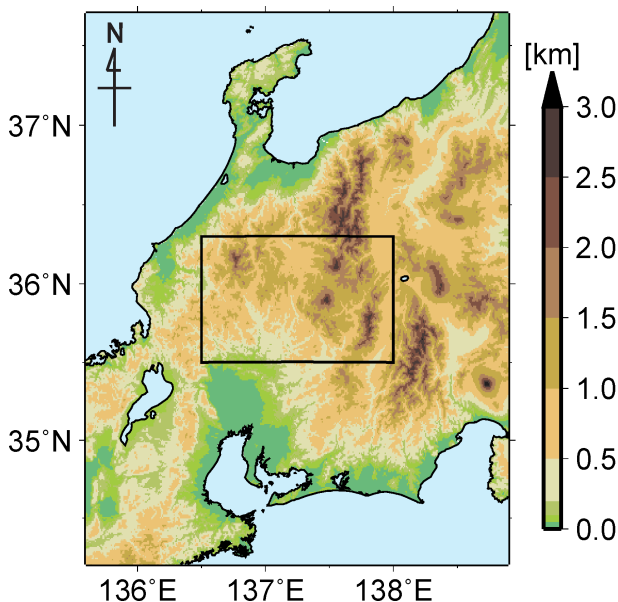


FIGURE A1 Box indicates the region that was used to calculate the amount of precipitation accumulated in 9 hr that occurred in 38 foehn cases with precipitation on windward slopes of mountains. The shaded field is terrain elevation [Colour figure can be viewed at wileyonlinelibrary.com]